Eur Phys J C **39**, s2, s1–s11 (2004)
Digital Object Identifier (DOI) 10.1140/epjcd/s2004-02-001-y

EPJ C direct
electronic only

Scientific Note:

Prospects for the detection of Kaluza-Klein excitations of gauge bosons in the ATLAS detector at the LHC

G. Azuelos[1] and G. Polesello[2]

[1] Université de Montréal, and TRIUMF (Vancouver), Canada
[2] INFN, Sezione di Pavia, Via Bassi 6, Pavia, Italy

Received: 20 March 2003 / Accepted: 20 August 2003 /
Published online: 10 March 2004 –

Abstract. Kaluza-Klein excitations of the gauge bosons are a notable feature of theories with "small" (~ 1 TeV) extra dimensions. The leptonic decays of the excitations of γ and Z bosons provide a striking signature which can be detected at the LHC. We investigate the reach for these signatures through a parametrized simulation of the ATLAS detector. With an integrated luminosity of 100 fb^{-1} a peak in the lepton-lepton invariant mass will be detected if the compactification scale (M_c) is below 5.8 TeV. If no peak is observed, with an integrated luminosity of 300 fb^{-1} a limit of $M_c < 12 - 13.5$ TeV can be obtained from a detailed study of the shape of the lepton-lepton invariant mass distribution. If a peak is observed, the study of the angular distribution of the two leptons will allow to distinguish the KK excitations from alternative models yielding the same signature. – 11.25Mj – 13.85-t

1 Introduction

In models with "large" extra dimensions, characterized by compactification radii $\gg 1/\text{TeV}$ [1], gravity propagates in the bulk, and the SM fields are confined to a 3-brane. The presence of the extra dimensions could be probed by searching for the Kaluza-Klein excitations of the gravitons at the future high energy accelerators, and these scenarios have been the subject of many phenomenological studies [2]. An interesting variation of the ADD model [3,4] assumes that only the fermions are confined in the 3-brane, whereas the gauge fields propagate also in a number of additional "small" extra dimensions orthogonal to the brane with compactification radius ~ 1 TeV^{-1}.

For definiteness we concentrate here on a model with only one "small" extra dimension, compactified on S^1/Z^2 and where all of the SM fermions are on the same orbifold point ($D = 0$). The phenomenology of this model, which we will label as M1 is discussed in some detail in [5]. The main signature is the appearance of a tower of KK resonances for each of the gauge fields propagating in the bulk. These resonances can be produced at future high energy colliders and detected through their decay to SM fermions. The model is completely specified by a single parameter M_c, the compactification scale, and the masses M_n of the KK modes of the gauge bosons are given by the relation $M_n^2 = (nM_c)^2 + M_0^2$, where M_0 is the mass of the zero-mode excitation corresponding to the Standard Model gauge boson. The couplings are the same as the corresponding SM couplings, scaled by a factor $\sqrt{2}$. As an example of variation on our reference model we also briefly consider an alternative model, [6] (M2), where quarks and leptons are at opposite fixed points. In this case the signs of the quark couplings of the bosons are reversed for excitations with n odd, yielding a somewhat different phenomenology.

The constraints on the compactification scale from precision electroweak measurements have been evaluated in a number of papers, [5],[7]-[13]. These studies estimate an approximate lower limit of 4 TeV on the compactification scale for the reference model considered in this analysis. A recent paper [14] calculates the limits which can be extracted from precision measurements at present high-energy accelerators. A 95% CL limit of 6.8 TeV is obtained, dominated by the LEP2 measurements. The limit, however, derives mainly from the fact that for two of the three fits to LEP data, an unphysical negative value for M_c is obtained, with a significance of two to three standard deviations. In view of this fact, waiting for a clarification of the claimed discrepancy with the Standard Model, we conservatively study the performance of the ATLAS detector starting from $M_c = 4$ TeV.

2 Signal simulation and data analysis

We simulate at particle level the production in pp interactions of the excitations of γ and Z, and their decay into leptons (e, μ), including the full interference and angular information. We include the full Breit-Wigner shape

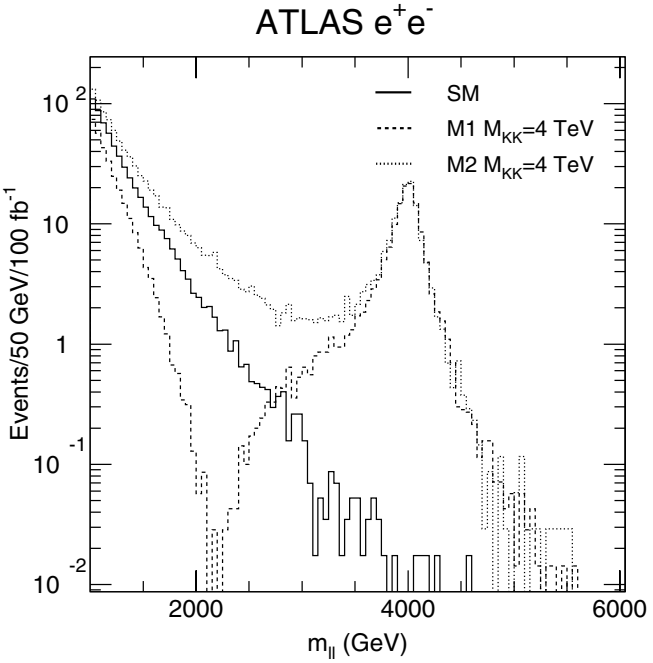

Fig. 1. Invariant mass distribution of e^+e^- pairs for the Standard Model (*full line*) and for models M1 (*dashed line*) and M2 (dotted line). The mass of the lowest lying KK excitation is 4000 GeV. The histograms are normalized to 100 fb^{-1}

for the first two excitations of γ and Z [15], and a resummed expression for the higher lying states, for which the approximation $M_n \gg \sqrt{\hat{s}}$ is used. Since the dominant contributions to the low $\hat{s}$ off-resonance region comes from the interference term between SM γ/Z and the KK excitations, the deviation from the SM is approximately proportional to:

$$\frac{1}{M_c^2}\sum_{n=1}^{\infty}\frac{1}{n^2} \tag{1}$$

Therefore the effect is increased by $\frac{\pi^2/6}{1.25} - 1 \sim 30\%$ when the full tower of resonances is considered instead of just the first two. If we consider model $M2$, the sum over the tower of resonances gives a term proportional to

$$\frac{1}{M_c^2}\sum_{n=1}^{\infty}(-1)^n\frac{1}{n^2} \;=\; -\frac{1}{2}\frac{1}{M_c^2}\sum_{n=1}^{\infty}\frac{1}{n^2}$$

Therefore, the summed contribution of the interference terms in model M2 will be of opposite sign and half of the one for the reference model. This is illustrated in Fig. 1, where the lepton-lepton invariant mass spectrum is shown respectively for model $M1$ (dashed line) and $M2$ (dotted line).

The matrix elements are interfaced to the PYTHIA 6.125 [16] event generator as an external process, and the generated events use the full PYTHIA machinery for QCD showering from the initial state quarks and for the hadronization. A set of events were produced with this program for proton-proton interactions at LHC energy (7+7 TeV colliding beams).

The events thus generated have been passed through the fast simulation of the ATLAS detector [17]. The lowest M_c considered in this study is 4 TeV. We therefore need to detect and measure leptons with momenta in the few TeV range. The energy resolution for electrons is in this case dominated by the constant term for calorimeter energy resolution. From measurements with particle beams and full simulation studies, this term has been measured to be a few per mil for energies up to a few hundred GeV. Additional studies are needed to extrapolate this result to the momentum range of interest here. With this caveat, we use in the analysis the standard parametrization included in the ATLFAST program which yields a resolution of $\sim$0.7% for the energy measurement of 2 TeV electrons. This is certainly optimistic, since electrons will radiate photons in the magnetic field of the inner detector. Such effects will have to be accounted for in the future when full simulation studies are available. However, given the fact that the peak resolution is dominated by the natural width of the bosons, the results are not affected by this approximation. More important for the analysis presented here is the level of understanding of the electron energy scale at such high momenta, which will be addressed in the following.

The transverse momentum measurement of high P_T muons is achieved through the sagitta measurement in drift chambers, and for a 2 TeV muon the resolution is of order 20%. The width of the lepton-lepton invariant mass distribution will therefore be dominated by the natural width for electrons, and by the experimental momentum resolution for muons. This is illustrated in Fig. 2 where the invariant mass spectra for a 4 TeV KK resonance is shown both for electrons (full line) and muons (dashed line). The statistics from both lepton flavors will be used in order to observe the existence of an excess in the peak region with respect to the Standard Model, but precision measurements will be restricted to the use of electrons.

Comparing the two-lepton invariant mass spectrum for Standard Drell-Yan production (full line), and for the reference model (dashed line) as shown in Fig. 1, two basic features can be observed:

- A peak centered around M_c, corresponding to the superposition of the $\gamma^{(1)}$ and $Z^{(1)}$ Breit-Wigner shapes.
- A suppression of the cross section with respect to the SM for masses below the resonance. This suppression is due to the negative interference terms between the SM gauge bosons and the whole tower of KK excitations, and is sizable even for compactification masses well above the ones accessible to a direct detection of the mass peak. This shape is the consequence of the model choices requiring both the leptons and the quarks to be at the same orbifold point (D=0). The different model choices corresponding to M2 would yield an enhancement of the off peak cross section, as shown in the dotted line in Fig. 1.

We select events with two isolated opposite sign leptons, satisfying the following requirements:

- $m_{\ell\ell} > 1000$ GeV ($\ell = e, \mu$)
- $p_T^{\ell} > 20$ GeV, $|\eta_{\ell}| < 2.5$

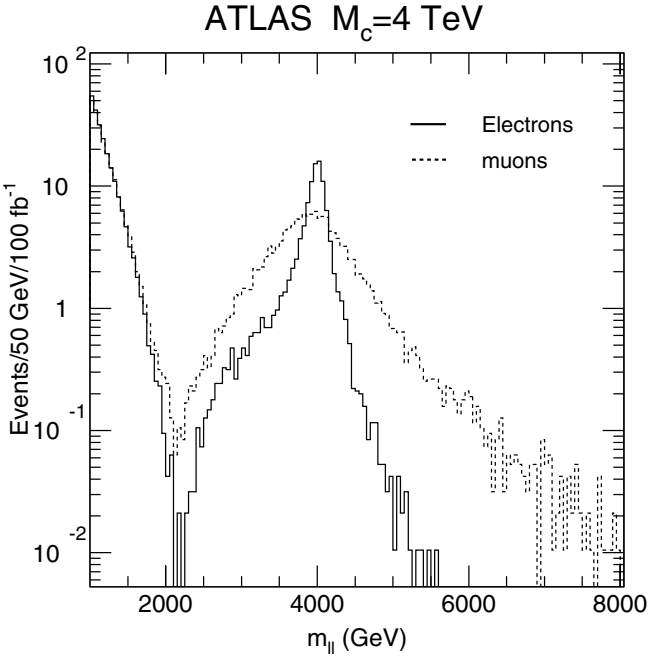

Fig. 2. Distribution of the lepton-lepton invariant mass for electrons (*full line*) and muons (*dashed line*). The distribution assumes 4 TeV for the mass the lowest lying KK excitation

The isolation criterion consists in requiring a transverse energy deposition in the calorimeter smaller than 10 GeV in a (η, ϕ) cone of radius 0.2 around the lepton direction, where η is the pseudorapidity, and ϕ the angle in the plane transverse to the beam. In the absence of new physics, approximately 500 events survive these cuts for an integrated luminosity of 100 fb^{-1}, corresponding to one year of high luminosity LHC operation for each of the lepton flavors. Besides the irreducible Drell-Yan background the following backgrounds were considered: $t\bar{t}$, WW WZ, and ZZ production. A total of approximately 70 events pass the cuts for each lepton flavour. Most of this background can be estimated from data and subtracted using lepton pairs with opposite flavours.

The reach for the observation of a peak in the $m_{\ell\ell}$ distribution can be naively estimated from Table 1, which, for both electrons and muons, gives the number of observed (N) and background (N_B) events for an integrated luminosity of 100 fb^{-1} for different values of M_c. As an arbitrary requirement for discovery we ask for the detection above a given $m_{\ell\ell}$ of 10 events summed over the two lepton flavors, and a statistical significance $(N - N_B)/\sqrt{N_B} > 5$. The lower bound on $m_{\ell\ell}$ is different for different values of M_c, and is chosen such as to retain as much as possible of the resonance width. The reach thus calculated is ∼5.8 TeV for an integrated luminosity of 100 fb^{-1}. A high $m_{\ell\ell}$ tail which might be produced by lepton momentum mismeasurement could endanger this result. The consideration of the momentum balance of the event in the transverse plane should allow to reject events with one badly mismeasured lepton.

Even for the lowest allowed value of M_c, 4 TeV, no events would be observed for the n=2 resonances of Z and γ at 8 TeV, which would have been the most striking signature for this kind of model.

Table 1. Expected number of events in the peak for an integrated luminosity of 100 fb^{-1}, for different values of the mass of the lowest lying KK excitation, and Standard Model background. The peak region is defined by requiring a minimum $\ell^+\ell^-$ invariant mass as shown in the second column. The results for electrons and muons are given separately

M_c(GeV)	Cut (GeV)	$N(e)$	$N(\mu)$	$N_B(e)$	$N_B(\mu)$
4000	3000	172	157	1.85	2.6
5000	4000	23	20	0.15	0.62
5500	4000	9	8	0.15	0.62
6000	4500	3.3	2.8	0.05	0.1
7000	5000	0.45	0.38	0.015	0.05
8000	6000	0.042	0.052	0.0015	0.012

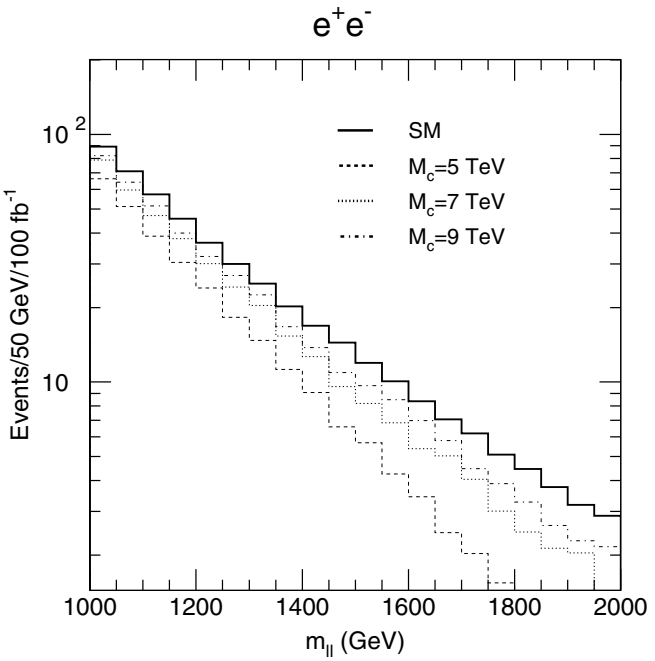

Fig. 3. Invariant mass distribution of e^+e^- pairs in the region below 2 TeV. The Standard Model contribution is shown as a thick line. We show the reference model with three different values for the compactification scale M_c: 5000, 7000 and 9000 GeV as *dashed, dotted* and *dash-dotted lines* respectively. The histograms are normalized to 100 fb^{-1}

As a first approach to the study of the off-peak region, one can simply evaluate the variation in the number of events within a given $m_{\ell\ell}$ range with respect to the SM, as a function of M_c. We show the invariant e^+e^- mass spectrum between 1000 and 2000 GeV in Fig. 3 for Standard Model and for three choices of M_c.

The statistical significance of the cross section suppression can again be naively parametrized as $(N-N_B)/\sqrt{N_B}$. A relevant variable which should also be considered is the ratio N/N_B, because the systematic uncertainty in our knowledge of the shape of $m_{\ell\ell}$ sets a limit on the detectable value of this ratio. The choice of the mass interval

Table 2. Expected number of events in the interference region for an integrated luminosity of 100 fb^{-1}, for different values of the compactification scale M_c and Standard Model e^+e^- background (1 lepton flavor). The considered mass interval is $1000 < m_{ee} < 2500$ GeV

M_c(GeV)	$N(e)$	M_c(GeV)	$N(e)$
SM	498	8000	420
4000	225	8500	428
5000	310	9000	434
5500	339	10000	447
6000	364	11000	458
7000	396	12000	465

is subject to the consideration of the systematical uncertainty, as the statistical significance somewhat increases by lowering the lower limit of the considered mass window, at the price of a worse N/N_B. We choose for this analysis the mass interval $1000 < m_{\ell\ell} < 2500$ GeV, and the corresponding number of observed events for background and signal for 100 fb^{-1} and one lepton flavour are given in Table 2. All the numbers in the table include a contribution of 15 events expected from reducible backgrounds. If we consider both lepton flavors, the ATLAS 5 σ reach is ∼8 TeV for an integrated luminosity of 100 fb^{-1} and ∼10.5 TeV for 300 fb^{-1}. The deviation from the Standard Model will be 15% for 8 TeV, and ∼ 10% for 10.5 TeV, defining in each case the level of systematic control on the relevant region of the lepton-lepton invariant mass spectrum we need to achieve to exploit the statistical power of the data.

3 Optimal reach and mass measurement

Instead of using just the invariant mass, one can use the full information contained in the events. Ignoring the transverse momentum of the $\ell^+\ell^-$ system, the event kinematics is fully defined by the variables $x_1, x_2, \cos\theta$, where x_i is the fraction of the proton momentum carried by parton i, and θ is the scattering angle in the partonic center of mass system. An optimal measurement of M_c can be obtained by a likelihood fit to the reconstructed distributions of these three variables. The values of x_1, x_2 can be evaluated from the four-momenta of the detected leptons, according to the formulas:

$$\frac{2\,P_L^{\ell\ell}}{\sqrt{s}} = x_1 - x_2, \quad m_{\ell\ell}^2 = x_1 x_2 s$$

For the evaluation of $\cos\theta$ we use the Collins-Soper convention [18], consisting in the equal sharing of the $\ell^+\ell^-$ system transverse momentum between the two quarks. A detailed discussion of the experimental reconstruction of the three variables is given in [19].

We perform the M_c estimation only for electrons, for which the unsmeared theoretical cross section expression can be used to build the unbinned likelihood function. For each input M_c value we generated an ensemble of Monte Carlo experiments (100 fb^{-1} each) and for each of them we estimated $1/M_c^2$ by maximizing the log-likelihood function.

Table 3. Average estimated value (M_L) and RMS of M_c for ∼ 2500 experiments and an integrated luminosity of 100 fb^{-1}

M_c(GeV)	M_L(GeV)	RMS
4000.	4002.0	10.9
5000.	5003.2	35.9
5500.	5502.2	77.2
6000.	6045.2	216.6
7000.	7129.5	544.4

The likelihood fit is performed on the variable $1/M_c^2$, since for $m_{\ell\ell} \ll M_c$ it is the natural variable for describing the deviation of the cross section from the Standard Model, as shown in (1). With the use of this test variable, the Standard Model is the limit corresponding to $1/M_c^2 = 0$, and it is possible to build a continuous likelihood function extending the evaluation to unphysical negative values of $1/M_c^2$.

We show in Fig. 4 the distributions of the estimated values of $1/M_c^2$ for two input values of M_c. As expected, the distributions are gaussian as long as events in the peak exist, and tails start to appear for M_c=6 TeV for which, on average, only three events appear in the peak region for the considered statistics. For M_c=7 TeV, less than 1 event is observed in the peak and the distribution becomes very broad, with an RMS corresponding to ∼600 GeV, and large tails. The average and RMS of the estimated value of M_c are given in Table 3. The statistical error is below the percent level as long as events are observed in the peak region. A small systematic shift in the average of the estimated M_c is observed, due to the fact that the likelihood is built using analytical test functions neglecting detector smearing and transverse motion of the e^+e^- system. The experimental sensitivity is defined in [20] as the average upper limit that would be attained by an ensemble of experiments with the expected background and no true signal. To evaluate the sensitivity, we therefore produced an ensemble of Monte Carlo experiments for which only SM Drell-Yan was generated. For each Monte Carlo experiment we built the likelihood function $\mathcal{L}$ as a function of $1/M_c^2$ as described above extending the fit interval to negative unphysical values of $1/M_c^2$. We then defined as 95% CL limit for each experiment as the value of M_c such that the integral of $\mathcal{L}$ between zero and $1/M_c^2$ is 95% of the integral between zero and infinity. This corresponds to a Bayesian prescription with uniform prior probability distribution function in the allowed region $1/M_c^2 > 0$. [21]. The experimental sensitivities for one lepton flavor thus obtained are respectively 9.5, 11 and 12 TeV for integrated luminosities of 100, 200 and 300 fb^{-1}. These values are conservative since they are not corrected for the positive systematic deviation from zero of the estimated $1/M_c^2$ value due to the approximate test function used. We verified that if this effect were corrected for the result would

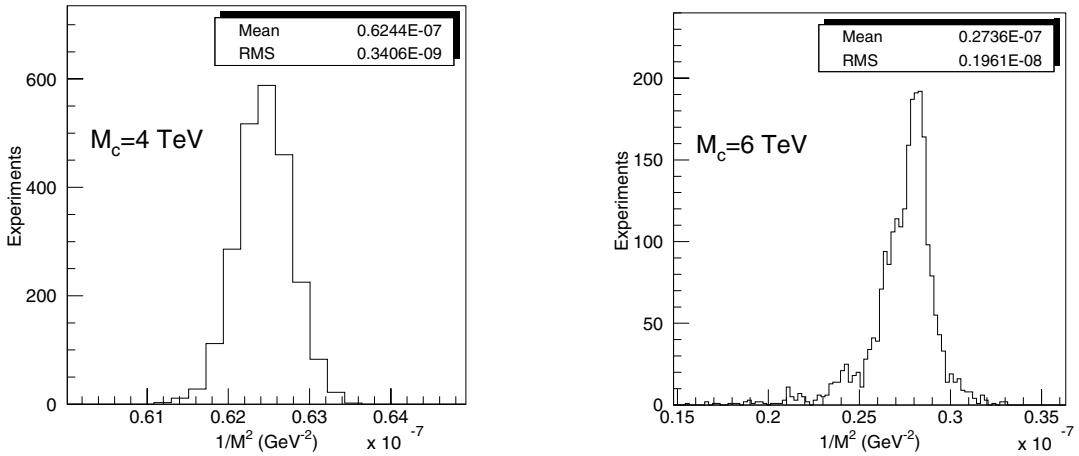

Fig. 4. Distribution of the value of $1/M_c^2$ estimated through the maximization of the likelihood function for a set of ∼1500 Monte Carlo experiments respectively for $M_c = 4$ TeV (*left plot*) and 6 TeV (*right plot*) The integrated luminosity is 100 fb^{-1}

improve by ∼200 GeV. If we assume similar sensitivity for electrons and muons, the sensitivity is ∼13.5 TeV for 300 fb^{-1} summing over the two lepton flavours. These figures only express the statistical sensitivity of the ATLAS experiment, the possible sources of systematic uncertainty must be considered as well.

4 Systematic uncertainties

As shown in the previous section, the effect of KK excitation can be detected for M_c well above the mass range for which the direct observation of a peak is possible. In order to exploit this sensitivity, we need a very good understanding of the expected kinematic distributions of the lepton-lepton system in the region $1000 < m_{ll} < 2500$ GeV. As shown in Fig. 3, as M_c increases, the difference in shape with respect to the Standard Model becomes less and less significant, and systematic uncertainties, both experimental and theoretical, may strongly affect the experimental sensitivity.

We expect the lepton energy scale to be the dominant experimental systematic uncertainty. At the TeV energy scale the linearity of the lepton momentum measurement, as well as the momentum dependence of the acceptance are difficult to assess using the data. In fact very few of the leptons from the decay of high momentum W and Z, which could in principle be used to perform the measurement will have high enough momentum. From studies performed for lepton calibration in ATLAS, we know that the lepton energy scale will be known to 0.1% at the Z mass. We therefore parametrize the deviation from linearity as a logarithmic term which is zero for lepton momentum of 100 GeV, and ±1% or ±5% for momenta of 2 TeV. We perform the likelihood analysis on all our simulated data samples, modifying event by event the reconstructed lepton energy according to the logarithmic formula. For the evaluation of M_c between 4 and 6 TeV, the relative deviation from the nominal M_c approximately follows the value of the deviation from linearity for 2 TeV leptons.

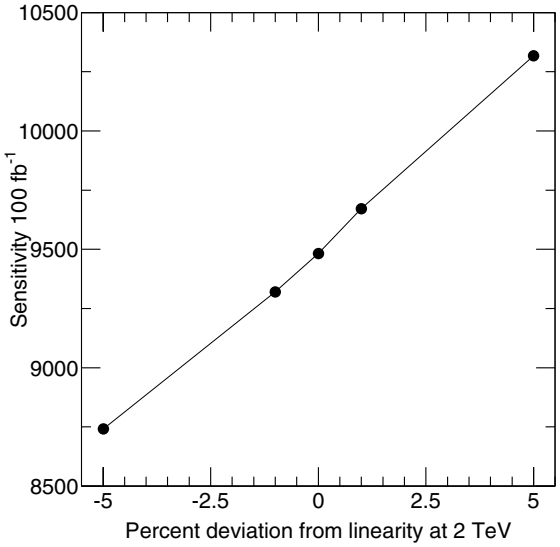

Fig. 5. Distribution of the expected sensitivity (100 fb^{-1}) in GeV as a function of the allowed deviation from linearity for electrons of 2 TeV momentum

The variation of the sensitivity with the assumed value of the deviation from linearity is shown in Fig. 5. The systematic uncertainty is reflected in a systematic shift of the average M_c estimate, and an overestimate of the lepton calibration is going to yield an optimistic evaluation of the M_c value excluded by the experiment. Taking the sensitivity values obtained with a negative deviation from linearity, the sensitivity for 100 fb^{-1} and one lepton species is reduced from 9.5 TeV to 9.3 TeV and 8.75 TeV for 1% and 5% deviation respectively. As an approximate rule, the experimental limit should be reduced by ∼2% for each percent of uncertainty on the energy calibration of 2 TeV leptons.

In the likelihood analysis we are not sensitive to the absolute normalization, but only to distortions of the kinematic distributions of the lepton-lepton system with respect to the SM. Therefore we do not consider uncertain-

ties on the K-factor or on luminosity determination. Three main sources of theoretical uncertainty can be identified:
- QCD higher order corrections;
- electroweak higher order corrections;
- the parton distribution function (PDF) for the proton.

The main effect of QCD higher order corrections is the modification of the p_T distribution of the lepton-lepton pair, due to radiation from initial state quarks. The likelihood function is built from the leading order 2-to-2 Drell-Yan expression, and the events are generated with the full PYTHIA machinery for initial state radiation. Therefore, the experimental error quoted in the previous section already includes a very pessimistic estimate of the uncertainty from this source.

Electroweak higher order corrections were recently calculated at NLO [22], and shown to be sizable, leading to a reduction of the cross section which varies with the lepton-lepton invariant mass, and can be as large as 35% for $pp \to \mu^+\mu^-$ and $m_{\mu^+\mu^-} > 1500$ GeV. The size of these corrections, which affect the background and signal in a similar manner, critically depends on the lepton identification and isolation criteria, as a substantial part of the higher order effects yield energetic photons produced alongside the leptons. The evaluation of the uncertainties on these corrections is thus a complex interplay of experimental and theoretical considerations which requires a dedicated study which is outside the scope of this analysis.

The shape of the kinematic distributions of the lepton-lepton system, in particular $m_{\ell\ell}$ has a strong dependence on the quark and antiquark PDF's in particular for high values of x. All the events were generated with the CTEQ4L PDF's [23]. In order to evaluate the effect of the uncertainty on the structure functions parametrization, the likelihood fit was performed on the generated data using a number of different structure function sets for the theoretical cross section formula. We have selected sets providing a leading order parametrization, and based on recent experimental data [24] [25] [26]. The distributions of estimated masses are shown in Fig. 6 for the eight choices of structure function sets used for $M_c = 4, 5$ and 5.5 TeV.

The systematic displacement from the true value is between 3 and 4 GeV for 4 TeV, increasing to 10-20 GeV for 5 TeV and 20-40 GeV for 5.5 TeV, and it is well below the RMS of the distributions given in Table 3. Another notable effect is that the quality of the likelihood fit is worse, giving rise to less gaussian distributions, and sizable tails start to appear for $M_c = 5.5$ TeV. The experimental reach for 100 fb^{-1} is shown in Fig. 7, as a function of the structure function set. In the worst case the reach is reduced by $\sim$ 200 GeV with respect to CTEQ4L.

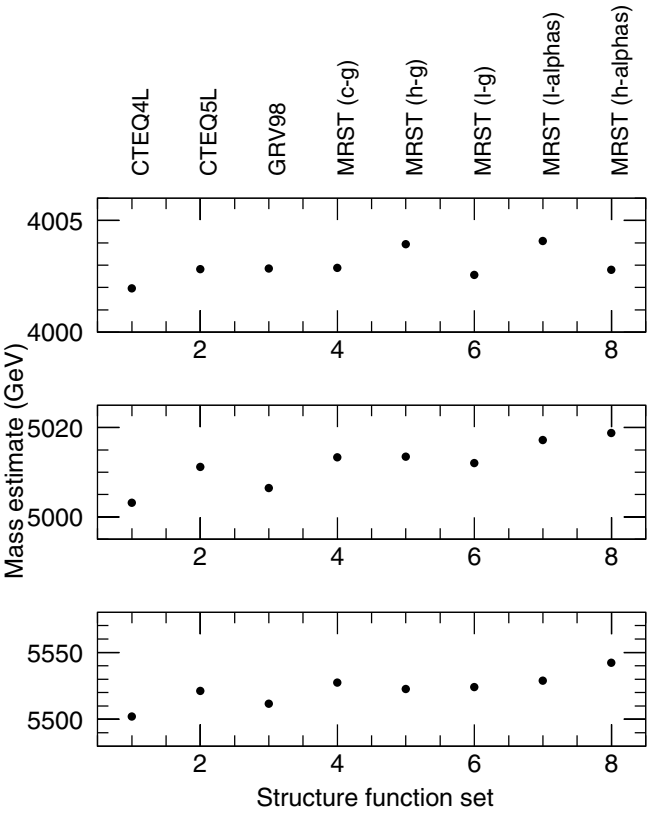

Fig. 6. Distribution of the measured values of M_c in GeV as a function of the structure function set used for the likelihood fit. The events were generated using CTEQ4L. The input values for M_c were respectively 4 TeV (*upper plot*) 5 TeV (*middle plot*) and 5.5 TeV (*lower plot*)

5 Angular distribution measurement

If a Kaluza-Klein gauge excitation is discovered, one of the ways of distinguishing the signal from a Z', predicted by GUT theories, or from a narrow graviton resonance G^* is by the angular distribution of the decay products, which should be consistent with the spin 1 nature of the excitation, and by the forward-backward asymmetry. By adjusting parameters of the models, the cross sections can be made comparable, but, as shown above and in [27], the shape of the mass distribution can provide an additional distinguishing criterion. The present study compares these distributions, but does not attempt to distinguish the resonances by the shape of their mass distributions, by their relative cross sections, nor by the branching ratios.

5.1 Cases studied

We studied the following cases
a) $Z^{(1)}/\gamma^{(1)}$: this is the case of gauge excitations, model M1 [5], at mass 4 TeV. The process was implemented in PYTHIA 6.201.
b) $Z^{(1)}/\gamma^{(1)}$-M2: this case of gauge excitation is with the alternative model M2 [6], also at 4 TeV. The process was implemented in PYTHIA.
c) Z': this is a standard model Z'. The same code as for case a) was used, but the first γ excitation and higher excitations of Z and γ were removed.
d) G^*: This is the case of a narrow graviton resonance, as was studied by [28]. The process is implemented in PYTHIA. In order to reproduce a resonance of width

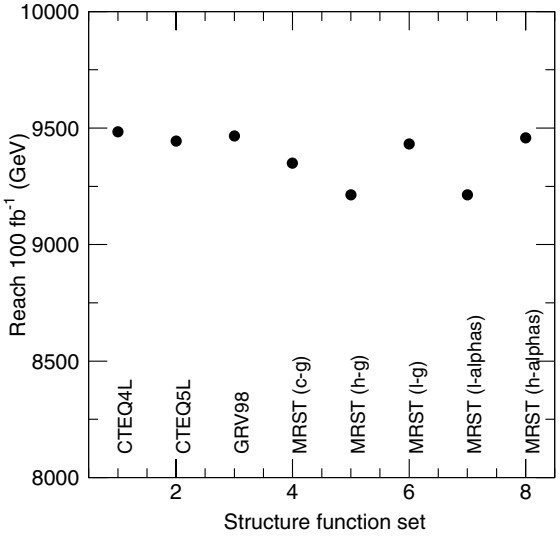

Fig. 7. Distribution of the expected sensitivity (100 fb^{-1}) in GeV as a function of the structure function set used for the likelihood fit. The events were generated using CTEQ4L

Table 4. Nominal cross sections of the different processes, after a preselection $\sqrt{\hat{s}} > 1$ TeV

process	$\sigma \times BR(Z^* \to e^+e^-)$ (fb)
$Z^{(1)}/\gamma^{(1)}$	4.05
$Z^{(1)}/\gamma^{(1)}$-M2	11.75
Z'	4.65
$qq \to G^*$	0.20
$gg \to G^*$	0.13
$qq \to e^+e^-$	4.83

comparable to the $Z^{(1)}/\gamma^{(1)}$ of a) above, the dimensionless coupling $\sqrt{2}x_1 k/M_{Pl}$ of the Randall-Sundrum model [29], where $x_1 = 3.83$ is the first zero of the J1 Bessel function and M_{Pl} is the modified Planck mass scale, was set to 0.8. The value of this constant and the mass of 4 TeV for this resonance are just outside the range of values suggested by [30] and represent, therefore, an extreme case. The reconstructed width is thus $\sigma \sim 82$ GeV. The angular distributions depend on the incoming partons. The two processes $qq \to G^* \to \ell^+\ell^-$ and $gg \to G^* \to \ell^+\ell^-$ were generated and added in proportion of their cross section. To their sum was added the Standard Model Drell-Yan background $qq \to Z/\gamma \to \ell\ell$.

The mass distributions normalized to a luminosity of 100 fb^{-1} are displayed in Fig. 8 for the different cases. The cross sections for the different processes are summarized in Table 4.

5.2 Angular distributions

As mentioned above, because the colliding particles at LHC are both protons, the forward-backward asymmetry is measured with some ambiguity. Given that the resonances are produced by $q\bar{q}$ fusion, the third component of the reconstructed momentum of the dilepton system is taken to be the quark direction, since the quark in the proton is expected to have higher energy than an antiquark from the sea.

Events around the peak of the resonance were selected: 3750 GeV $< m_{ee} <$ 4250 GeV or 3250 GeV $< m_{\mu\mu} <$ 4750 GeV. For these events, the cosine of the angle of the lepton, with respect to the beam direction, in the frame of the decaying resonance, is shown in Fig. 9, for the electron channel. The positive direction was defined by the sign of the reconstructed momentum of the dilepton system. For the high lepton momenta involved, the sign of the charge can be incorrectly reconstructed, leading to about 15% loss of events. The probability of wrong charge assignment for electrons and muons, evaluated in [31] was therefore folded in. Since we are interested only in the shape, and not in the cross sections, the angular distribution histograms have been normalized, to a total of 116 events (123 for muons), corresponding to the number of events predicted with an integrated luminosity of 100 fb^{-1} for the reference case $Z^{(1)}/\gamma^{(1)}$.

To compare the shape of these distributions, a set of 1000 angular distributions from the different types of resonances was generated by sampling from the expected distributions of Fig. 9. A Kolmogorov test was then applied[1] between the expected $Z^{(1)}/\gamma^{(1)}$ distribution and distributions sampled from the other resonances. The result of the test is expected to be a uniform distribution between 0 and 1 if they come from the same parent distribution. The histogram of the result is displayed in Fig. 10. No significant difference is found between models M1 and M2 of $Z^{(1)}/\gamma^{(1)}$, as expected. However, the Kolmogorov test, applied to the distributions obtained for the e^+e^- channel, will give an average probability of consistency between $Z^{(1)}/\gamma^{(1)}$ and Z' or between $Z^{(1)}/\gamma^{(1)}$ and G^* of 0.13 and 0.028 respectively and will reject, at 95% confidence level, the hypothesis that the distributions derive from the same parent distribution 45% and 91% of the times. For higher resonance masses the statistical significance quickly decreases: at 5 TeV, with only 18 events in the peak region, no discrimination becomes possible. However, for this mass but with an integrated luminosity of 300 fb^{-1}, the Kolmogorov test would reject the hypothesis, at 95% CL, about 15% of the times. Similar results are obtained for the $\mu^+\mu^-$ channel.

A χ^2 test was also performed between these distributions, leading to the same conclusions. Here, also, a histogram of the calculated χ^2 was produced from a sample of 1000 pseudo experiments with 116 events each. The average χ^2/d.f. are 1.05, 1.53 and 2.1 (20 d.f.) for the cases of model M2, Z' and G^* respectively. The goodness of fit test between the $Z^{(1)}/\gamma^{(1)}$ and the Z' or G^* angular distributions would yield a confidence level below 5% respectively 42% and 77% of the times.

[1] In principle, the Kolmogorov test should be applied on unbinned data, but the application on binned data should still provide a valid test in the present case since the bins are narrower than the expected features.

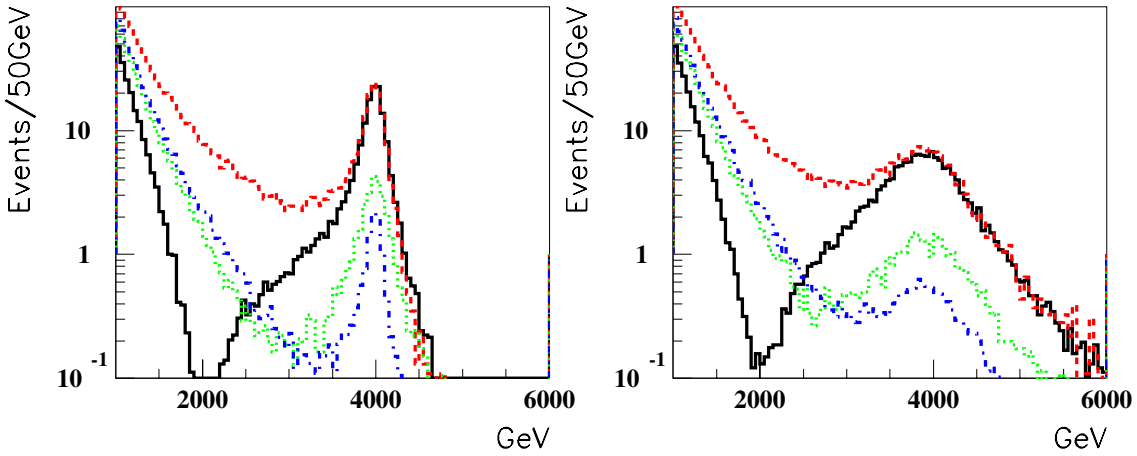

Fig. 8. Mass distributions of the resonances considered: *left:* electron channel; *right:* muon channel; (i) *black full line*, $Z^{(1)}/\gamma^{(1)}$, (ii) *red dashed line*, $Z^{(1)}/\gamma^{(1)}$ model M2, (iii) *dotted green line*, Z', (iv) *dash-dotted blue line*, G^*+ SM Drell-Yan

5.3 Forward-backward asymmetry

From the angular distributions, the forward-backward asymmetry is obtained and shown in Figs. 11 as a function of the reconstructed dilepton mass. It allows a clear distinction between a resonance due to $Z^{(1)}/\gamma^{(1)}$ and either a Z' or a G^* resonance. Indeed, the asymmetry is expected to be close to 0 at the mass peak of the Z', if the couplings are those of the SM, because $\sin^2\theta_W \sim 1/4$:

$$A^0_{FB} = \frac{3}{4} A_q A_\ell \qquad \text{with}$$
$$A_\ell = \frac{2v_\ell a_\ell}{v_\ell^2 + a_\ell^2} = \frac{2(1-4|Q_\ell|\sin^2\theta_W)}{1+(1-4|Q_\ell|\sin^2\theta_W)^2} \sim 0$$

For masses below, but close to the resonance, the FB asymmetry can also serve as a distinguishing criterion between the Z' and the $Z^{(1)}/\gamma^{(1)}$. For large masses, however, the discrimination power becomes quickly limited by statistics.

6 Conclusions

We have performed a detailed study of the leptonic signatures for the production of the Kaluza-Klein excitations of the γ and Z in models with TeV-scale extra dimensions.

The production and decay of the excitations were fully simulated, including initial state QCD radiation, and the resulting particles were passed through a parametrized simulation of the ATLAS detector.

We found that with an integrated luminosity of 100 fb^{-1} ATLAS will be able to detect a peak in the lepton-lepton invariant mass if the compactification scale (M_c) is below 5.8 TeV. Even in the absence of a peak, a detailed study of the shape of the lepton-lepton invariant mass will allow to observe a deviation from the Standard Model due to the interference of the KK excitations with the SM bosons. From a study based on a maximum likelihood estimation of the compactification mass, ATLAS will be able to exclude at 95% CL a signal from the models considered in this work for $M_c < 12-13.5$ TeV with an integrated luminosity of 300 fb^{-1}. We have performed an evaluation of the influence of experimental and theoretical uncertainties on this result. A 1% deviation from linearity in lepton momentum measurement yields a 2% reduction in sensitivity. The maximum effect observed from the consideration of various sets of PDF's is a reduction of order 200 GeV on the achievable limit.

Once a peak is observed, an important question is the assessment of the model which has produced the signal. We show that for resonances of mass up to $\lesssim$5 TeV, and with an integrated luminosity of 300 fb^{-1}, the KK excitations can be distinguished from mass peaks produced by SM-like Z' or graviton resonances from the study of the polar angle distribution of the leptons in the peak region. The forward-backward lepton asymmetry as a function of invariant mass can provide a more general distinguishing criterion among the different models. For invariant masses around the peak, it will allow to distinguish the KK excitations from alternative models yielding the same signature.

Acknowledgements. We warmly thank the organisers of the Les Houches 2001 workshop, where the present study was started. We thank Tom Rizzo for proposing the topic to us, and for useful discussions. This work has been performed within the ATLAS collaboration, and we thank collaboration members for helpful discussions. We have made use of the physics analysis and simulation tools which are the result of collaboration-wide efforts. This work has been supported by the Natural Sciences and Engineering Research Council of Canada, and by INFN, Italy.

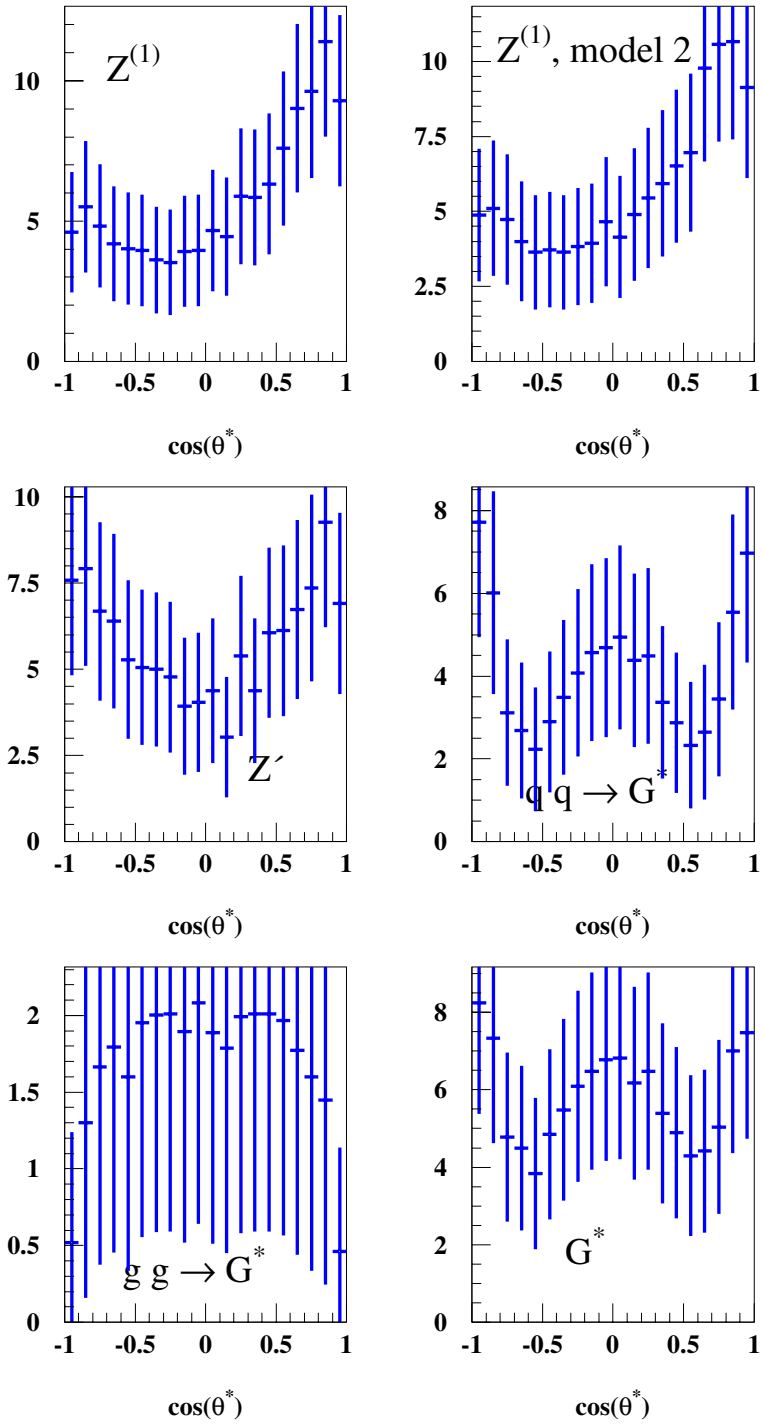

Fig. 9. Electron channel: angular distributions for the different types of resonances considered. The distributions are normalized to a total of 116 events in the peak and therefore the error bars indicate the expected scatter of the measurements. The distribution labelled G^* is made up of contributions from the distributions labelled $qq \to G^*$ and $gg \to G^*$

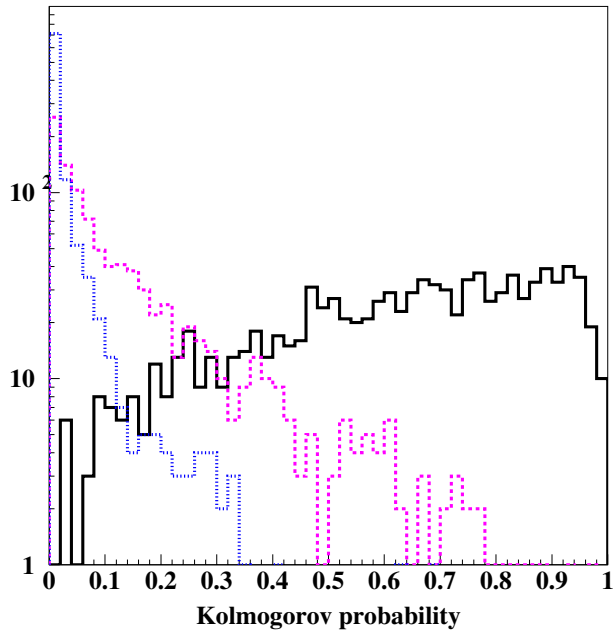

Fig. 10. Kolmogorov probability from comparison of $Z^{(1)}/\gamma^{(1)}$ angular distribution with (i) *black full line:* model M2, (ii) *pink dashed line:* Z' and (iii) *blue dotted line:* G^*. A histogram is constructed from 1000 pseudo samples of events

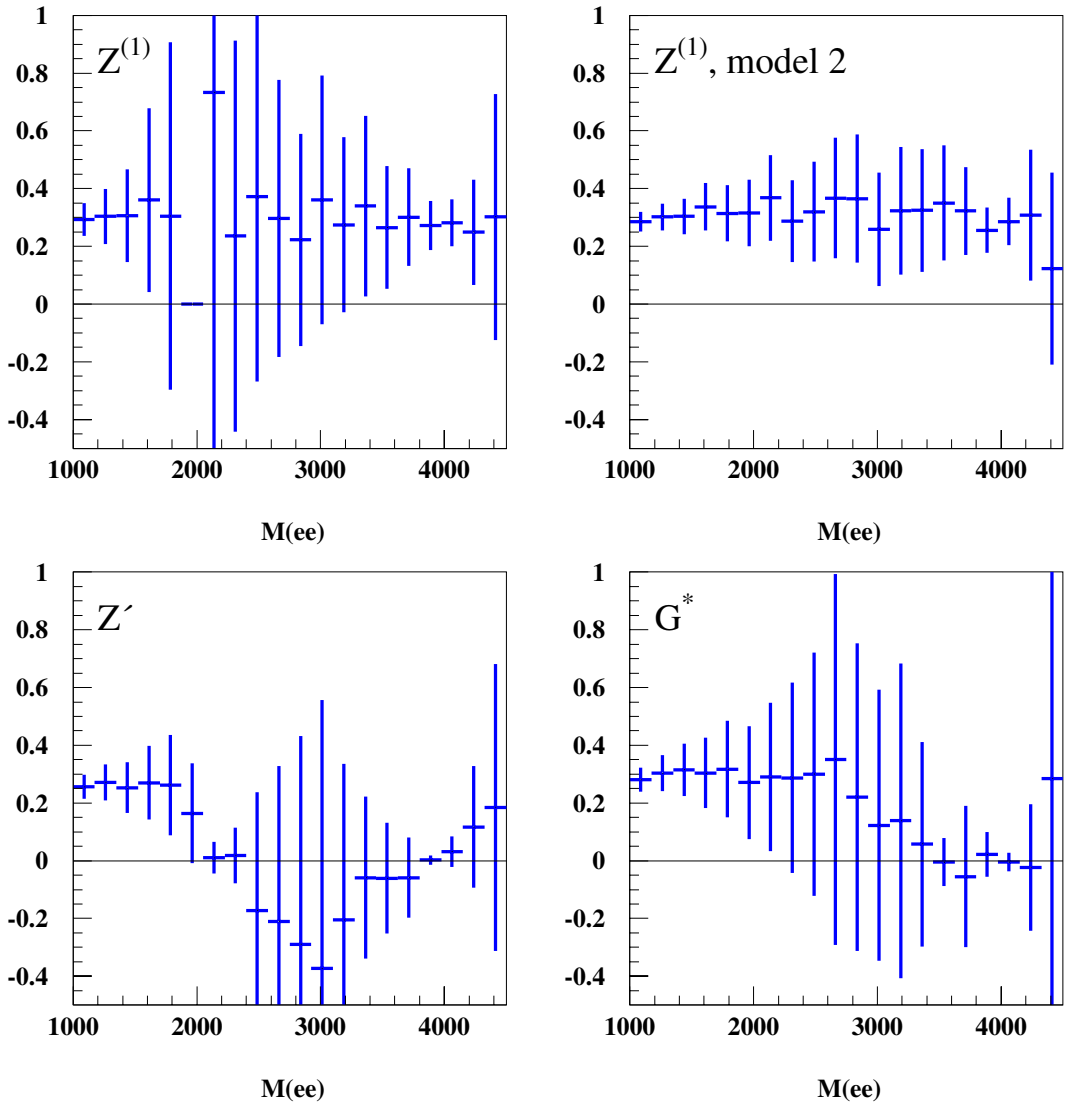

Fig. 11. Electron channel: measured forward-backward asymmetry at LHC, for different types of resonances, centered at m = 4 TeV. The error bars are representative of a sample having 116 events in the peak region, or 100 fb^{-1} for $Z^{(1)}/\gamma^{(1)}$

References

1. N. Arkani-Hamed, S. Dimopoulos, G. Dvali: Phys. Lett. B **249**, 263 (1998)
   Phys. Rev. D **59**, 086004 (1999)
2. For a summary of the very extensive literature on the subject, see: J.A. Hewett, M. Spiropulu: *Particle Physics Probes of Extra Spacetime Dimensions,* hep-ph/0205106, and references therein
3. K. Dienes, E. Dudas, T. Gherghetta: Nucl. Phys. B **537**, 47 (1999)
4. A. Pomarol, M. Quirós: Phys. Lett. B **438**, 255 (1998); M. Masip, A. Pomarol: Phys. Rev. D **60**, 096005 (1999); I. Antoniadis, K. Benakli, M. Quirós: Phys. Lett. B **460**, 176 (1999)
5. T.G. Rizzo: Phys. Rev. D **61**, 055005 (2000)
6. N. Arkhani-Hamed, M. Schmalz: Phys. Rev. D **61**, 033005 (2000)
7. P. Nath and M. Yamaguchi: Phys. Rev. D **60**, 116004 (1999)
   P. Nath, Y. Yamada, M. Yamaguchi: Phys. Lett. B **466**, 100 (1999)
8. T. Rizzo, J. Wells: Phys. Rev. D **61**, 016007 (2000)
9. R. Casalbuoni, S. Curtis, D. Dominici, R. Gatto: Phys. Lett. B **462**, 48 (1999)
10. A. Strumia: Phys. Lett. B **466**, 107 (1999)
11. C. Carone: Phys. Rev. D **61**, 015008 (2000)
12. A. Delgado, A. Pomarol, M. Quirós: JHEP **0001**, 030 (2000)
13. F. Cornet, M. Relaño, and J. Rico: Phys. Rev. D **61**, 037701 (2000)
14. K. Cheung, G. Landsberg: Phys. Rev. D **65**, 076003 (2002)
15. We warmly thank Tom Rizzo for providing us with the FORTRAN code for Z/γ excitations production and for the help in implementing it
16. T. Sjöstrand: Comp. Phys. Comm. series **82**, 74 (1994)
17. E. Richter-Was, D. Froidevaux, L. Poggioli: *ATLFAST 2.0: a fast simulation package for ATLAS*, ATLAS Internal Note ATL-PHYS-98-131 (1998)
18. J. Collins, D. Soper: Phys. Rev. **16**, 2219 (1977)
19. D. Choudhury, R. Godbole, G. Polesello: JHEP **0208**, 004 (2002)
20. G.J. Feldman, R.D. Cousins: Phys. Rev. D **57**, 3873 (1998)
21. D.E. Groom et al., Particle Data Group: *Review of Particle Physics*, Eur. Phys. J. C. **15** (2000)
22. U. Baur, O. Brein, W. Hollik, C. Schappacher, D. Wackeroth: Phys. Rev. D **65**, 033007 (2002)
23. H.L. Lai, J. Huston, S. Kuhlmann, F. Olness, J. Owens, D. Soper, W.K. Tung, H. Weerts: Phys. Rev. D **55**, 1280 (1997)
24. H.L. Lai, J. Huston, S. Kuhlmann, J. Morfin, F. Olness, J. Owens, J. Pumplin, W.K. Tung: Eur. Phys. J. C **12**, 375 (2000)
25. M. Glück, E. Reya, A. Vogt: Eur. Phys. J. C **5**, 461 (1998)
26. A.D. Martin, R.G. Roberts, W.J. Stirling, R.S. Thorne: Eur. Phys. J. C **4**, 463 (1998)
27. T. Rizzo: *Distinguishing Kaluza-Klein Resonances From a Z' in Drell-Yan Processes at the LHC*, hep-ph/0109179
28. B.C. Allanach, K. Odagiri, M.A. Parker, B.R. Webber: JHEP **0009**, 019 (2000)
    B.C. Allanach, K. Odagiri, M.J. Palmer, M.A. Parker, A. Sabetfakhri, B.R. Webber: JHEP **0212**, 039 (2002)
29. L. Randall, R. Sundrum: Phys. Rev. Lett. **83**, 3370 (1999)
30. H. Davoudiasl, J.L. Hewett, T.G. Rizzo: Phys. Rev. D **63**, 075004 (2001)
31. *Inner Detector Technical Design Report*, ATLAS Collaboration, CERN/LHC/97-16